

HEPSY 97-01
June 1997

THE BTeV PROGRAM

SHELDON STONE

*Physics Department, 201 Physics Building, Syracuse University,
Syracuse, NY 13244-1130, USA*

A brief description is given of BTeV a proposed program at the Fermilab collider sited at the C0 intersection region. The main goals are measurement of mixing, CP violation and rare decays in both the b and charm systems. The detector is a two arm forward-backward spectrometer capable of triggering on detached vertices and dileptons, and possessing excellent particle identification, electron, photon and muon detection.

.....
*Presented at "B Physics and CP Violation," Honolulu, Hawaii, March 1997;
to appear in the proceedings.*

1 Introduction

BTeV is a Fermilab collider program whose main goals are to measure mixing, CP violation and rare decays in the b and c systems. Using the new Main injector, now under construction, the collider will produce on the order of 10^{11} b hadrons in 10^7 sec. of running. This compares favorably with e^+e^- colliders operating at the $\Upsilon(4S)$ resonance. These machines, at their design luminosities of $3 \times 10^{33} \text{cm}^{-2}\text{s}^{-1}$ will produce 6×10^7 B mesons in 10^7 seconds.¹

2 Importance of Heavy Quark Decays

The physical point-like states of nature that have both strong and electroweak interactions, the quarks, are mixtures of base states described by the Cabibbo-Kobayashi-Maskawa matrix:²

$$\begin{pmatrix} d' \\ s' \\ b' \end{pmatrix} = \begin{pmatrix} V_{ud} & V_{us} & V_{ub} \\ V_{cd} & V_{cs} & V_{cb} \\ V_{td} & V_{ts} & V_{tb} \end{pmatrix} \begin{pmatrix} d \\ s \\ b \end{pmatrix} \quad (1)$$

The unprimed states are the mass eigenstates, while the primed states denote the weak eigenstates. A similar matrix describing neutrino mixing is possible if the neutrinos are not massless.

There are nine complex CKM elements. These 18 numbers can be reduced to four independent quantities by applying unitarity constraints and the fact that the phases of the quark wave functions are arbitrary. These four remaining numbers are fundamental constants of nature that need to be determined from experiment, like any other fundamental constant such as α or G . In the Wolfenstein approximation the matrix is written as³

$$V_{CKM} = \begin{pmatrix} 1 - \lambda^2/2 & \lambda & A\lambda^3(\rho - i\eta) \\ -\lambda & 1 - \lambda^2/2 & A\lambda^2 \\ A\lambda^3(1 - \rho - i\eta) & -A\lambda^2 & 1 \end{pmatrix}. \quad (2)$$

The constants λ and A have been measured.⁴

The phase η allows for CP violation. CP violation thus far has only been seen in the neutral kaon system. If we can find CP violation in the B system we could see if the CKM model works or perhaps go beyond the model. Speculation has it that CP violation is responsible for the baryon-antibaryon asymmetry in our section of the Universe. If so, to understand the mechanism of CP violation is critical in our conjectures of why we exist.⁵

Unitarity of the CKM matrix leads to the constraint triangle shown in Fig. 1. The leftside can be measured using charmless semileptonic b decays,

while the rightside can be measured by using the ratio of B_s to B_d mixing. The angles can be found by measuring CP violating asymmetries in hadronic B decays.

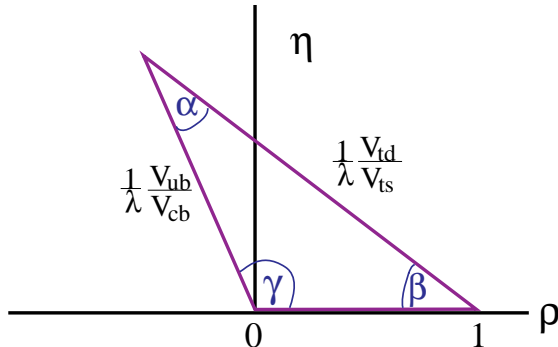


Figure 1: The unitarity triangle shown in the $\rho - \eta$ plane. The left side is determined by measurements of $b \rightarrow u/b \rightarrow c$ and the right side can be determined using mixing measurements in the B_s and B_d systems. The angles can be found by making measurements of CP violating asymmetries in hadronic B decays.

The current status of constraints on ρ and η is shown in Fig. 2. One constraint on ρ and η given by the K_L^0 CP violation measurement (ϵ),⁶ where the largest error arises from theoretical uncertainty. Other constraints come from current measurements on V_{ub}/V_{cb} , and B_d mixing.⁴ The width of both of these bands are also dominated by theoretical errors. Note that the errors used are $\pm 1\sigma$. This shows that the data are consistent with the standard model but do not pin down ρ and η .

It is crucial to check if measurements of the sides and angles are consistent, i.e., whether or not they actually form a triangle. The standard model is incomplete. It has many parameters including the four CKM numbers, six quark masses, gauge boson masses and coupling constants. Perhaps measurements of the angles and sides of the unitarity triangle will bring us beyond the standard model and show us how these parameters are related, or what is missing.

3 The Main Physics Goals of BTeV

3.1 Physics Goals For B 's

Here I briefly list the main physics goals for studies of the b quark.

- Precision measurements of B_s mixing, both the time evolution x_s and the lifetime difference, $\Delta\Gamma$, between the positive CP and negative CP final states.

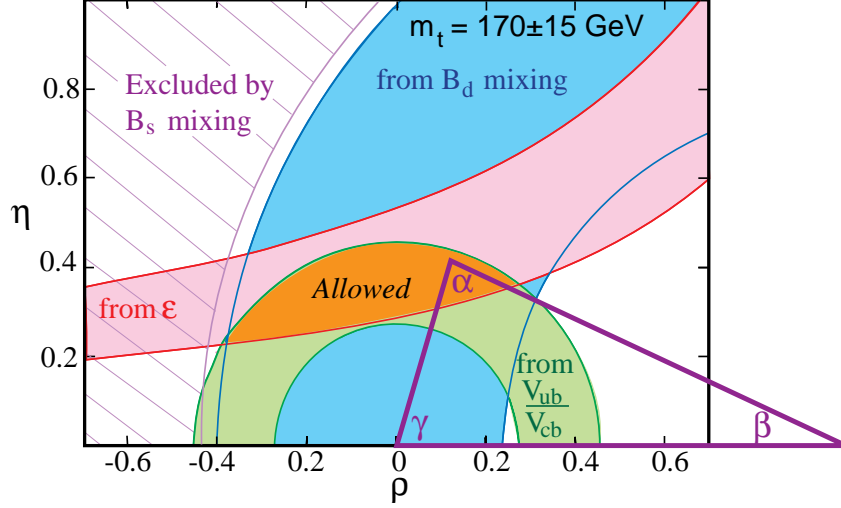


Figure 2: The regions in $\rho-\eta$ space (shaded) consistent with measurements of CP violation in K_L^0 decay (ϵ), V_{ub}/V_{cb} in semileptonic B decay, B_d^0 mixing, and the excluded region from limits on B_s^0 mixing. The allowed region is defined by the overlap of the 3 permitted areas, and is where the apex of the CKM triangle sits. The bands represent $\pm 1\sigma$ errors. The error on the B_d mixing band is dominated by the parameter f_B . Here the range is taken as $240 > f_B > 160$ MeV.

- Measurement of the “CP violating” angles α and γ . We will use $B^0 \rightarrow \pi^+\pi^-$ for α and measure γ using several different methods including $B^+ \rightarrow D^0 K^+$, $B^+ \rightarrow \bar{D}^0 K^+$, where the D^0 can decay directly or via a doubly Cabibbo suppressed decay mode. We also need measure the conjugate B^- decay modes.^{7,8}
- Search for rare final states such as $K\mu^+\mu^-$ and $\pi\mu^+\mu^-$ which could result from new high mass particles coupling to b quarks.
- We assume that the CP violating angle β will have already been measured by using $B^0 \rightarrow \psi K_s$, but we will be able to significantly reduce the error.

3.2 The Main Physics Goals for charm

According to the standard model, charm mixing and CP violating effects should be “small.” Thus charm provides an excellent place for non-standard model effects to appear. Specific goals are listed below.

- Search for mixing in D^0 decay, by looking for both the rate of wrong sign decay, r_D and the width difference between positive CP and negative CP eigenstate decays, $\Delta\Gamma$. The current upper limit on r_D is 3.7×10^{-3} , while the standard model expectation is $r_D < 10^{-7}$.⁹

- Search for CP violation in D^0 . Here we have the advantage over b decays that there is a large D^{*+} signal which tags the initial flavor of the D^0 through the decay $D^{*+} \rightarrow \pi^+ D^0$. Similarly D^{*-} decays tag the flavor of initial \bar{D}^0 . The current experimental upper limits on CP violating asymmetries are on the order of 10%, while the standard model prediction is about 0.1%.¹⁰

- Search for direct CP violation in charm using D^+ and D_s^+ decays.
- Search for rare decays of charm, which if found would signal new physics.

3.3 Other b and charm Physics Goals

There are many other physics topics that can be addressed by BTeV. A short list is given here.

- Measurement of the $b\bar{b}$ production cross-section and correlations between the b and the \bar{b} in the forward direction.
- Measurement of the B_c production cross-section and decays.
- The spectroscopy of b baryons.
- Precision measurement of V_{cb} using the usual mesonic decay modes the baryonic decay mode $\Lambda_b \rightarrow \Lambda_c \ell^- \bar{\nu}$ to check the form-factor shape predictions.
- Precision measurement of V_{ub}/V_{cb} using the baryonic decay modes $\Lambda_b \rightarrow p \ell^- \bar{\nu}$ and $\Lambda_b \rightarrow \Lambda_c \ell^- \bar{\nu}$ and the usual mesonic decay modes.
- Measurement of the $c\bar{c}$ production cross-section and correlations between the c and the \bar{c} in the forward direction.
- Precision measurement of V_{cd} and the form-factors in the decays $D \rightarrow \pi \ell^+ \nu$ and $D \rightarrow \rho \ell^+ \nu$.
- Precision measurement of V_{cs} and the form-factors in the decay $D \rightarrow K^* \ell^+ \nu$.

4 Characteristics of Hadronic b Production

It is often customary to characterize heavy quark production in hadron collisions with the two variables p_t and η . The later variable was first invented by those who studied high energy cosmic rays and is assigned the value

$$\eta = -\ln(\tan(\theta/2)), \quad (3)$$

where θ is the angle of the particle with respect to the beam direction.

According to QCD based calculations of b quark production, the b 's are produced "uniformly" in η and have a truncated transverse momentum, p_t , spectrum, characterized by a mean value approximately equal to the B mass.¹¹ The distribution in η is shown in Fig. 3.

There is a strong correlation between the B momentum and η . Shown also in Fig. 3 is the $\beta\gamma$ of the B hadron versus η . It can clearly be seen that near

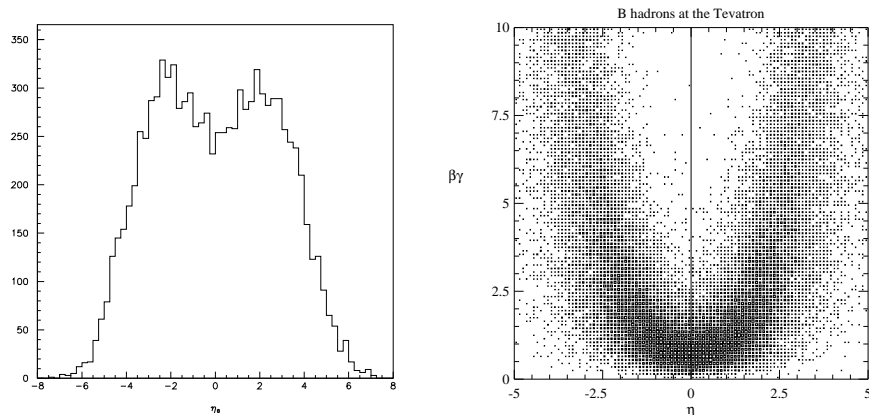


Figure 3: The B yield versus η (left). $\beta\gamma$ of the B versus η (right).

η of zero, $\beta\gamma \approx 1$, while at larger values of $|\eta|$, $\beta\gamma$ can easily reach values of 6. This is important because the observed decay length varies with $\beta\gamma$ and furthermore the absolute momenta of the decay products are larger allowing for a suppression of the multiple scattering error.

Since the detector design is somewhat dependent on the Monte Carlo generated b production distributions, it is important to check that the correlations between the b and the \bar{b} are adequately reproduced. In Fig. 4 I show the azimuthal opening angle distribution between a muon from a b quark decay and the \bar{b} jet as measured by CDF¹² and compare with the MNR predictions.¹³

The model does a good job in representing the shape which shows a strong back-to-back correlation. The normalization is about a factor of two higher in the data than the theory, which is generally true of CDF b cross-section measurements.¹⁴ In hadron colliders all B species are produced at the same time.

The “flat” η distribution hides an important correlation of $b\bar{b}$ production at hadronic colliders. In Fig. 5 the production angles of the hadron containing the b quark is plotted versus the production angle of the hadron containing the \bar{b} quark according to the Pythia generator. There is a very strong correlation in the forward (and backward) direction: when the B is forward the \bar{B} is also forward. This correlation is not present in the central region (near zero degrees). By instrumenting a relative small region of angular phase space, a large number of $b\bar{b}$ pairs can be detected. Furthermore the B ’s populating the forward and backward regions have large values of $\beta\gamma$.

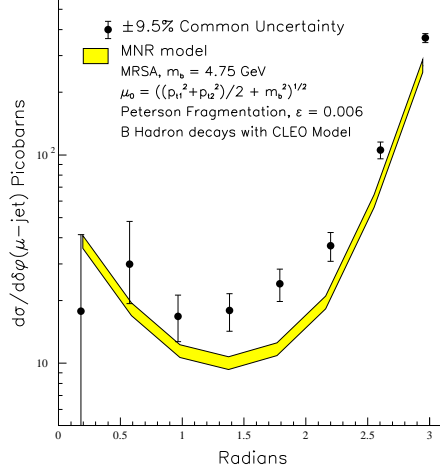


Figure 4: The differential $\delta\phi$ cross-sections for $p_T^\mu > 9$ GeV/c, $|\eta^\mu| < 0.6$, $E_T^{\bar{b}} > 10$ GeV, $|\eta^{\bar{b}}| < 1.5$ compared with theoretical predictions. The data points have a common systematic uncertainty of $\pm 9.5\%$. The uncertainty in the theory curve arises from the error on the muonic branching ratio and the uncertainty in the fragmentation model.

Charm production is similar to b production but much larger. Current theoretical estimates are that charm is 1-2% of the total $p\bar{p}$ cross-section. Table 1 gives the relevant Tevatron parameters. We expect to start serious data taking in Fermilab Run II with a luminosity of about $5 \times 10^{31} \text{cm}^{-2} \text{s}^{-1}$; our ultimate luminosity goal, to be obtained in Run III is $2 \times 10^{32} \text{cm}^{-2} \text{s}^{-1}$.

5 The Experimental Technique: A Forward Two-arm Spectrometer

A sketch of the apparatus is shown in Fig. 6. The plan view shows the two-arm spectrometer fitting in the expanded C0 interaction region at Fermilab. There is a construction money in the budget for excavating the interaction region and installing a counting room. The magnet that we will use, called SM3, exists at Fermilab. The other important parts of the experiment include the vertex detector, the RICH detectors, the EM calorimeters and the muon system.

The solid angle subtended is approximately ± 300 mr in both plan and elevation views. The vertex detector is a multiplane pixel device which sits inside the beam pipe. The triggering concept is to pipeline the data and to trigger on detached b or c vertices in the first trigger level. The vertex detector is put in the magnetic field in order to insure that the tracks considered for vertex based triggers do not have large multiple scattering because they are low momentum.

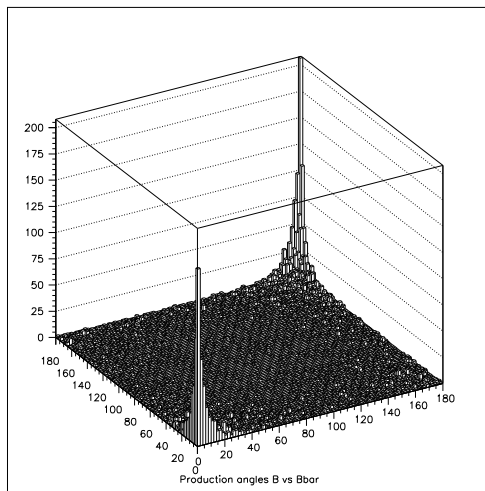


Figure 5: The production angle (in degrees) for the hadron containing a b quark plotted versus the production angle for a hadron containing \bar{b} quark.

6 Simulations

We have developed several fast simulation packages to verify the basic BTeV concepts and aid in the final design. The key program in our system is MCFast.¹⁵ Charged tracks are generated and traced through different material volumes including detector resolution, multiple scattering and efficiency. This allows us to measure acceptances and resolutions in a fast reliable manner.

Our baseline trigger algorithm works by first determining the main event vertex and then finding how many tracks miss this vertex by $n\sigma$, where σ refers to the impact parameter divided by its error. Furthermore, a requirement is then placed on the track momentum in the bend plane, p_y , as determined on line. The preliminary results of simulating this algorithm are shown in Fig. 7 for a cut $p_y > 0.5$ GeV/c.¹⁶ The choice of the number of tracks and the impact parameter requirement must eventually be fixed, but what is shown here (left) is the efficiency for accepting light quark events (u , d , and s) for various choices on the number of tracks (curves) and the size of their required impact parameter divided by the error in impact parameter. The efficiency for accepting $B^0 \rightarrow \pi^+\pi^-$ is shown in the right side. Here the efficiency is given after requiring that both tracks are in the spectrometer and accepted for further analysis. For a “typical” $n\sigma$ cut of 3 and track requirement of 2, the $\pi^+\pi^-$ trigger efficiency is about 45%, while The light quark background has an

Table 1: The Tevatron as a b and c source for C0 in Run II.

Luminosity in Run II	$5 \times 10^{31} \text{cm}^{-2} \text{s}^{-1}$
Luminosity (ultimate)	$2 \times 10^{32} \text{cm}^{-2} \text{s}^{-1}$
b cross-section	$100 \mu\text{b}$
# of b 's per 10^7 sec	10^{11}
b fraction	0.2%
c cross-section	$> 500 \mu\text{b}$
Bunch spacing	132 ns
Luminous region length	$\sigma_z = 30 \text{ cm}$
Luminous region length	$\sigma_x \sigma_y = \approx 50 \mu\text{m}$
Interactions/crossing	$< 0.5 >$

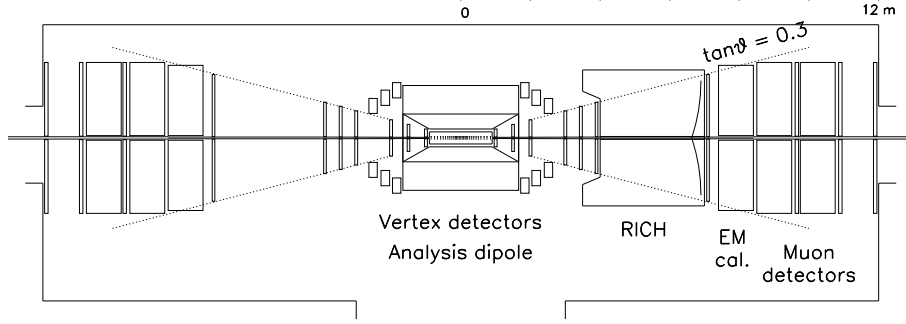


Figure 6: Sketch of the BTeV spectrometer.

efficiency of about 0.8%. Note, that we do not consider c to be a background in this experiment. For “typical” charm reaction the same trigger gives about a 1% efficiency on charm.

For the $B^0 \rightarrow \pi^+\pi^-$ channel we have also compared the offline fully reconstructed decay length distributions in our forward geometry with that of detector configured to work in the central region using MCFAST. In Fig. 8 I show the normalized decay length expressed in terms of L/σ where L is the decay length and σ is the error on L for the $B^0 \rightarrow \pi^+\pi^-$ decay.¹⁷

The forward detector clearly has a much more favorable L/σ distribution, which is due to the excellent proper time resolution. This will be crucial for studies of B_s mixing. For the decay mode $B_s^0 \rightarrow \psi K^{*0}$ our proper time resolution is 45 fs, which allows us to measure values of x_s up to 50 in several

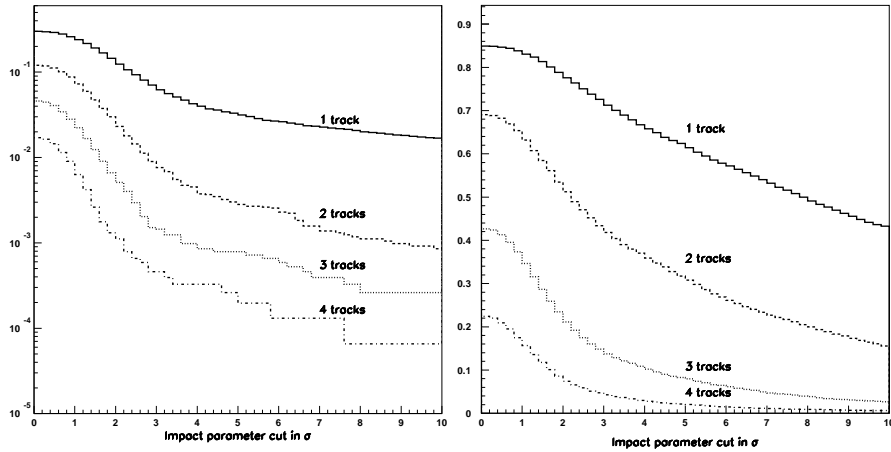


Figure 7: (left) Trigger efficiency for light quark events. (right) Trigger efficiency for $B^0 \rightarrow \pi^+\pi^-$ for pion tracks in the spectrometer. The ordinate gives the choice of cut value on the impact parameter in terms of number of standard deviations (σ) of the track from the primary vertex. The curves show the effect of requiring different numbers of tracks.

years of running.

We have also investigated the feasibility of tagging kaons using a gas Ring Imaging Cherenkov Counter (RICH) in a forward geometry and compared it with what is possible in a central geometry using Time-of-Flight counters with good, 100 ps, resolution. For the forward detector the momentum coverage required is between 3 and 70 GeV/c. The lower momentum value is determined by our desire to tag charged kaons for mixing and CP violation measurements, while the upper limit comes from distinguishing the final states $\pi^+\pi^-$, $K^+\pi^-$ and K^+K^- . The momentum range is much lower in the central detector but does have a long tail out to about 5 GeV/c. Either C₄F₁₀ or C₅F₁₂ have pion thresholds of about 2.5 GeV/c. The kaon and proton thresholds for the first gas are 9 and 17 GeV/c, respectively.

The BTeV RICH was simulated using the current C0 geometry with MC-Fast. Fig. 9 shows the number of identified kaons plotted versus their impact parameter divided by the error in the impact parameter for both right sign and wrong sign kaons. A right sign kaon is a kaon which properly tags the flavor of the other B at production. We expect some wrong sign kaons from mixing and charm decays. Many others just come from the primary. A cut on the impact parameter standard deviation plot at 3.5σ gives an overall ϵD^2 of 6%. Here ϵ is

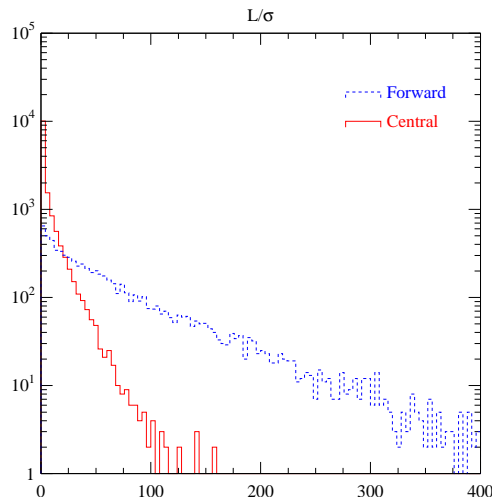


Figure 8: Comparison of the L/σ distributions for the decay $B^0 \rightarrow \pi^+\pi^-$ in central and forward detectors produced at a hadron collider with a center of mass energy of 1.8 TeV.

the efficiency and D is the dilution which can be expressed as number of right sign minus the number of wrong sign divided by the sum. The 6% may be an over-estimate because protons can contribute to the sample. Putting these in lowers ϵD^2 to 5.1%. These numbers are for a perfect RICH system. Putting in a fake rate of several percent, however, does not significantly change this number.

The simulation of the central detector gives much poorer numbers. In Fig. 9 ϵD^2 for both the forward and central detectors are shown as a function of the kaon impact parameter (protons have been ignored). It is difficult to get ϵD^2 of more than 1.5% in the central detector. This analysis showed the importance of detecting protons so we are now in the process of seeing if we can provide low momentum K/p separation using another radiator.

7 Conclusions

Progress has been made toward starting a program to measure mixing, CP violation and rare decays in both the b and c systems at the Fermilab collider. The pit at the C0 collision hall is being enlarged and can accomodate a two-

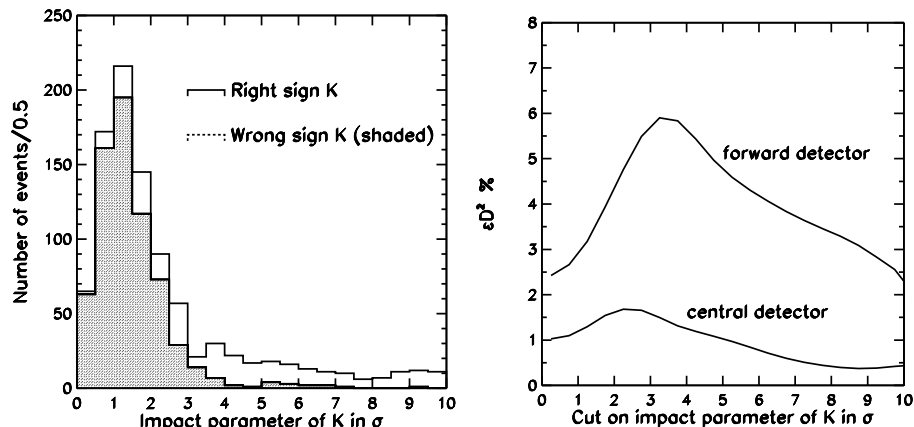


Figure 9: (left) L/σ distributions in BTeV for K^\pm impact parameters for right sign (unshaded) and wrong sign (shaded) tags. (right) Overall ϵD^2 values from kaon tagging for a forward detector containing a fluorine based RICH versus a central detector with 100 ns time of flight resolution as a function of kaon impact parameter in units of L/σ . (Protons have been ignored in both cases.)

arm forward spectrometer as described above. The BTeV collaboration hopes to start taking data, with at least a portion of the apparatus during collider Run II at about the same time the Tevatron changes to 132 ns bunch spacing, although test runs are expected well before. The full spectrometer is hoped for in collider Run III. The detector design incorporates detached vertex triggering at the first level with excellent tracking and charged particle identification using a Ring Imaging Cherenkov system. It also has separate elements for electron and muon detection.¹⁹

The enormous potential physics power of the experiment is reflected by how well we can expect to measure the CP violating asymmetry in the decay $B^0 \rightarrow \pi^+\pi^-$. Table 2 gives the relevant parameters. In one year of “low” luminosity running the asymmetry can be measured to an accuracy of ± 0.05 .

Acknowledgments

I would like to thank my BTeV colleagues including Joel Butler, Chuck Brown and Patty McBride, Tomasz Skwarnicki and Kevin Sterner for their help in getting this material together.

Table 2: The Tevatron as a b and c source for C0 in Run II.

Luminosity	$5 \times 10^{31} \text{cm}^{-2} \text{s}^{-1}$
b cross-section	$100 \mu\text{b}$
Number of B_d^0 's	3.5×10^{10}
$\mathcal{B}(B_d^0 \rightarrow \pi^+ \pi^-)$	0.75×10^{-5}
Reconstruction efficiency	0.09
Trigger efficiency	0.72
Number reconstructed $\pi^+ \pi^-$	1.7×10^4
Tagging Efficiency ϵD^2	0.10
Signal/Background	0.40
error in asymmetry	0.05

References

1. The CESR B Physics Working Group, K. Lingel *et al*, "Physics Rationale For a B Factory", Cornell Preprint CLNS 91-1043 (1991); SLAC Preprint SLAC-372 (1991); "Progress Report on Physics and Detector at KEK Asymmetric B Factory," KEK Report 92-3 (1992)
2. N. Cabibbo, *Phys. Rev. Lett.* **10**, 531 (1963); M. Kobayashi and K. Maskawa, *Prog. Theor. Phys.* **49**, 652 (1973).
3. L. Wolfenstein, *Phys. Rev. Lett.* **51**, 1945 (1983).
4. S. Stone, "Prospects For B-Physics In The Next Decade," presented at *NATO Advanced Study Institute on Techniques and Concepts of High Energy Physics*, Virgin Islands, July 1996, to be published in proceedings.
5. P. Langacker, "CP Violation and Cosmology," in *CP Violation*, ed. C. Jarlskog, World Scientific, Singapore p 552 (1989).
6. A. J. Buras, "Theoretical Review of B-physics," in *BEAUTY '95* ed. N. Harnew and P. E. Schlein, *Nucl. Instrum. Methods* **A368**, 1 (1995).
7. M. Gronau and D. Wyler, *Phys. Lett. B* **265**, 172 (1991).
8. D. Atwood, I. Dunietz and A. Soni, *Phys. Rev. Lett.* **78**, 3257 (1997).
9. Private communication from I. Bigi and G. Burdman.
10. M. Golden and B. Grinstein *Phys. Lett. B* **222**, 501 (1989); F. Buccella *et al*, *Phys. Rev. D* **51**, 3478 (1995).
11. M. Artuso, "Experimental Facilities for b-Quark Physics," in *B Decays* revised 2nd Edition, Ed. S. Stone, World Scientific, Sinagapore (1994).
12. F. Abe *et al*, *Phys. Rev. D* **53**, 1051 (1996).
13. M. Mangano, P. Nason and G. Ridolfi, *Nucl. Phys. B* **373**, 295 (1992).
14. F. Abe *et al*, *Phys. Rev. Lett.* **75**, 1451 (1995). Previous UA1 measure-

- ments agreed with the theoretical predictions, see C. Albajar *et al*, *Phys. Lett. B* **256**, 121 (1991). Recent D0 measurements agree with both the CDF measurements and the high side of the theoretically allowed range. See S. Abachi *et al*, *Phys. Rev. Lett.* **74**, 3548 (1995).
15. P. Avery *et al*, "MCFast: A Fast Simulation Package for Detector Design Studies," Presented at The International Conference on Computing in High Energy Physics, Berlin 1997. To appear in the proceedings.
 16. These results are based on the work of R. Isik, W. Selove, and K. Sterner, "Monte Carlo Results for a Secondary-vertex Trigger with On-line Tracking," Univ. of Penn. preprint UPR-234E (1996).
 17. M. Procario, "*B* Physics Prospects beyond the Year 2000," invited talk at 10th Topical Workshop on Proton-Antiproton Physics, Fermilab-CONF-95/166 (1995).
 18. P. McBride and S. Stone, *Nucl. Instr. and Meth.* A368, 38 (1995).
 19. For more information on BTeV please see <http://fnsimu1.fnal.gov/btev.html>